ELSEVIER

Polymer 43 (2002) 4651–4655

polymer

www.elsevier.com/locate/polymer

Microviscosity of an ion-conducting polymer probed by fluorescence depolarization and dielectric spectroscopy

Sangmin Jeon, Sung Chul Bae, Jeff Turner, Steve Granick*

Department of Materials Science and Engineering, University of Illinois, Urbana, IL 61801, USA

Received 16 March 2002; received in revised form 2 May 2002; accepted 8 May 2002

Abstract

The local segmental motions of polypropylene oxide melt with variable amounts of added $LiClO_4$ salt (0.3–2.2 mol% per repeat unit) were studied using dielectric relaxation spectroscopy and single photon counting methods after two-photon excitation of an unattached fluorescent dye, rhodamine123, embedded at low concentration within the polymer. The lithium ions serve as junctions between polymer chains and increase the bulk viscosity. The measured microviscosity contains information on the local environment of ClO_4^- ions. © 2002 Elsevier Science Ltd. All rights reserved.

Keywords: Ion conducting polymer; Dielectric spectroscopy; Fluorescence depolarization

1. Introduction

It is well known that polyethers such as polyethylene oxide, polypropylene oxide (PPO), and polytetramethylene oxide show high DC conductivity after addition of alkali metal ions. The polyether dissolves alkali metal salts and its dissociated alkali metal ions are tetrahedrally coordinated by polyether oxygen. Although the conduction mechanism is unclear, it is generally accepted that the dissociated metal cations contribute to DC conductivity by achieving mobility through the micro-Brownian motion of polymer segments [1,2]. Conversely, the dissociated anions move independently of the polymer motion [3]. These ion-conductive polymers have been studied extensively mainly because of their importance in industrial applications such as a polymer battery. That is why most studies to date have focused on the motion of ions [4–9]. However, this polymer electrolyte also has potential as a medium for electrochemical processes and it is important to study the local environment of the polymer within which the ions are embedded.

Among the polyethers, PPO has some interesting features. It is an amorphous flexible polymer that possesses a strong dipole along the chain dipole and another significant component perpendicular to it. Therefore, it displays characteristic relaxation peaks in both directions when a sinusoidal electric field is applied [10]. The backbone relaxation, so called normal mode relaxation, is usually hidden by segmental mode relaxation especially if the molecular weight is less than 1000 g mol^{-1}. Also, the glass transition temperature of PPO is unusually insensitive to molecular weight; it shows no dependence on molecular weight down to 400 g mol^{-1} [10]. This absence of free ends effect is attributed to the hydrogen bonding which reduces the mobility of free ends. This hydrogen bonding effect was confirmed by replacing oxygen with sulfur, which is incapable of hydrogen bonding [11]. Unlike PPO, polypropylene sulfide shows the expected significant decrease of glass transition temperature for lower mass.

Recently we studied the dielectric response of thin films of PPO with added $LiClO_4$ confined between atomically-smooth surfaces of mica [12]. Significant retardation of polymer motion and decrease of conductivity were observed when it was confined to thickness <100 nm. Although the conductivity depends on the mobility of ions and this again depends on the motion of polymer, the local environment of PPO that surrounds the ions has not previously been studied, as far as we know. We used here a combination of time-resolved two photon excited fluorescence anisotropy and dielectric relaxation spectroscopy to understand the local motions of positive ions and negative ions.

* Corresponding author.
E-mail address: sgranick@uiuc.edu (S. Granick).

PII: S0032-3861(02)00317-8

2. Experimental **setup

2.1. Time-resolved fluorescence depolarization

Time-resolved fluorescence depolarization is a method to quantify rotational relaxation times on the nanosecond time scale. In this way, rotational motions of a fluorescent molecule are used to probe the local microenvironment within which it resides.

Two-photon excitation of the fluorescent probe molecules was induced using a femtosecond Ti/Sapphire laser (Mai Tai, Spectra-physics) whose FWHM (full-width at half-maximum) pulse was measured to be 100 fs. The repetition rate was 80 MHz and the wavelength was 800 nm. The experiments were performed within a homemade microscope designed to combine this measurement with the surface forces apparatus (SFA). However, a perfusion chamber (Sigma) with 1.3 mm total thickness was used in these initial experiments in order to simplify the surface geometry.

In the design that we employed, the vertically-polarized laser beam was first split into two beams and one of them was introduced into an objective lens (Mitutoyo; numerical aperture, NA = 0.55) and focused onto the sample. The other beam was used as a trigger signal for the single photon counting system (Becker & Hickl GmbH, Berlin, Germany). The emitted fluorescence was collected by the same objective lens and focused again by a tube lens in order to increase the response of the photomultiplier tube (PMT) detectors. A fast PMT (Hamamatsu, R5600) and a photodiode were used to detect the fluorescence and the trigger signal, respectively. The PMT signal was input to the time-to-amplitude converter as a start signal followed by a constant fractional discriminator (Becker & Hickl GmbH, TCSPC730). In this setup the total instrument response function was around 150 ps. The instrument and measurement protocol have been described in detail elsewhere [13].

2.2. Dielectric measurements

Dielectric relaxation measurements employed a Solartron 1260 gain-phase impedance Analyzer connected to a Solartron 1296 dielectric interface. Its frequency range is, in principle, from one micro Hz to three million Hz. Since the relaxations of interest here appeared at frequencies above 100 Hz, measurements were made starting at 1 Hz. A homebuilt thermoelectric stage and water circulator (RTE211, Neslab) were used for temperature control in the anisotropy and dielectric relaxation measurements, respectively. Temperature was controlled to $\pm 0.1\,^{\circ}C$. Sufficiently thin mica allowed Ag electrodes to be sputter-deposited onto the backside, using methods standard in the SFA technique [12–15]. The resulting electrode is shielded from the sample by the mica dielectric, which is atomically smooth and clean because it was freshly cleaved shortly before the experiment. Furthermore, it is possible to avoid strong electrode polarization owing to this dielectric mica buffer. However, it presents the disadvantage that the capacitance 'empty cell' (the mica-coated electrodes) varies from experiment to experiment and therefore cannot be calibrated in order to convert the measured capacitance to dielectric permittivity [15].

When the response to sinusoidal input electric field at frequency f is decomposed into one component in-phase with the field, and a second component in-phase with its rate of change, the former (real) component is dominated by the mica buffer sheets between the electrodes and sample. The latter (loss) component, $C''(f)$, contains an immeasurably small contribution from the mica sheets and reflects only the sample [15]. In principle, it is possible to evaluate the dielectric permittivity from experimentally measured values, but this requires accurate calibration of the empty cell (bare mica capacitance). In our current experimental setup it was not possible to perform these experiments in an atmosphere sufficiently dry to obtain a sufficiently reliable evaluation of C_m (mica–mica contact). The influence of moisture condensed on the mica surfaces became plain when measurements were performed in nominal mica–mica contact (two cleaved mica sheets placed in contact). The ratio C''/C' was variable between experiments, as discussed elsewhere [15]. There then resulted a large uncertainty in the capacitance of the two mica layers and it was not possible to be confident that C_m measured for mica–mica contact remained the same after sample was added. Therefore, in the results that follow, the raw data $C'(f)$ and $C''(f)$ will be presented. Because the out-of-phase contribution of the sample cell (mica) to $C''(f)$ was negligible [15], its frequency dependence is believed to have been the same as for the PPO samples of interest.

2.3. Materials

The polymer (PPO), the fluorescent dye (rhodamine123) and the salt ($LiClO_4$) were purchased from Aldrich and used as received. As given by the manufacturer, the PPO samples had number-average molecular weight $M_n = 3500\ g\ mol^{-1}$. The glass transition temperature is around 200 K. Spectroscopic grade methanol was bought from Mellinckrodt and used as received. For complete mixing, all materials were dissolved in methanol. After vigorous stirring with a vortex mixer, solvent was evaporated at 80 °C under low pressure for 8 h. Complete drying was confirmed by measuring the total mass before and after evaporation. The concentration of rhodamine123 in this experiment was 16 μM, which corresponds to the ratio of one probe molecule to one million PPO repeating units. Lithium ion concentration was varied from 0.33 to 2.18 mol% of ion per PPO repeating unit. Watanabe et al. [7] have shown that the conductivity increases up to 1% of Li^+ ions but decreases at higher concentrations owing to the increase of viscosity.

3. Results and discussion

Fig. 1 contrasts the dielectric relaxation of PPO with and without added salt at several temperatures. Complex capacitance, in-phase with the drive ($C'(f)$), and 90° out-of-phase with the drive ($C''(f)$), are plotted against frequency of the applied electric field. The top panel shows the real value of the capacitance, while the middle and bottom panels refer to the imaginary response without and with added $LiClO_4$, respectively. When salt was added

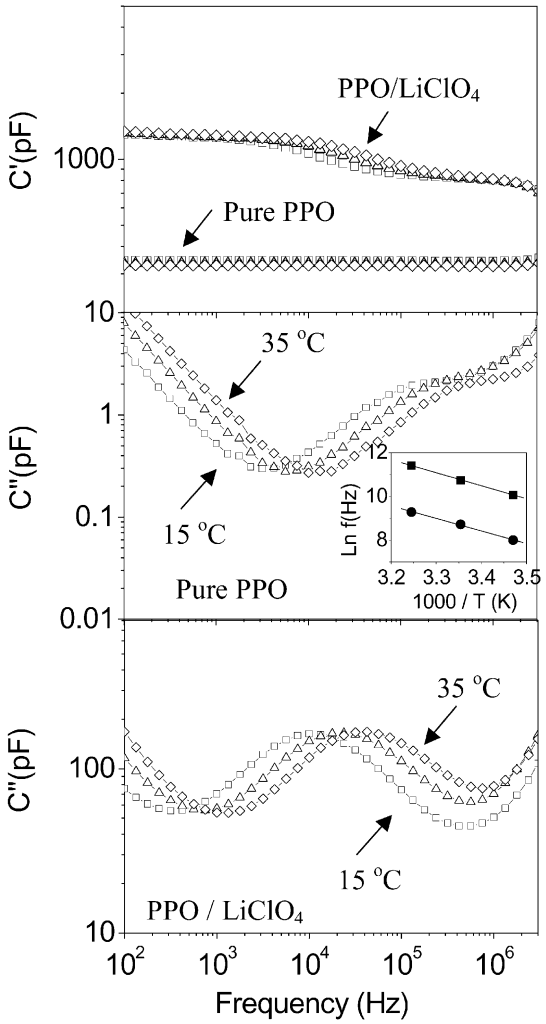

Fig. 1. For several temperatures, dielectric relaxation spectra of PPO melt and of PPO melt with added $LiClO_4$ are plotted on log–log scales against frequency of the oscillatory electric field. The top panel shows the real capacitance, in-phase with drive. The middle panel shows the imaginary capacitance (90° out-of-phase with the drive) from pure PPO melt. The bottom panel shows the imaginary capacitance from PPO with 1% Li^+/PPO repeating unit. The temperature was 15 °C (squares), 25 °C (triangles), and 35 °C (diamonds). The inset shows an Arrhenius plot summarizing the imaginary responses; the logarithmic peak frequency of the relaxation corresponding to normal motion is plotted against inverse temperature, for pure PPO melt (■) and PPO with 1% $LiClO_4$ (•). Since the segmental mode relaxation did not appear fully here within the available frequency window, temperature-induced shifts of the low-frequency side of normal mode relaxation were considered for quantifying the activation energy.

to PPO, its real capacitance increased by an order of magnitude compared to pure PPO and showed an inflection near $f = 10\,000$ Hz owing to relaxation of lithium ions at this frequency.

The middle panel of Fig. 1, showing the imaginary response of pure PPO, shows three regimes. At the lowest frequencies ($<10^4$ Hz), the upturn reflects DC conductivity. At intermediate frequencies ($<8\times10^5$ Hz), the peak reflects relaxation of the end-to-end vector between dipoles along the PPO chain. At the highest frequencies ($<3\times10^6$ Hz), one sees contributions from local segmental motions. In order to avoid overlap with this latter peak, when quantifying the activation energy for relaxation of the end-to-end vector we considered temperature-induced shifts of the low-frequency side of that process.

Notice the larger ordinate scale in the bottom panel of Fig. 1. The bottom panel of Fig. 1 shows that when salt was added, the DC conductivity shifted to still lower frequencies and a huge new relaxation peak appeared at intermediate frequencies. This peak, reflecting ionic motion, screened the normal mode peak. Segmental mode relaxation at still higher frequency was not fully visible within the available frequency range but Furukawa [6] has shown that the segmental mode relaxation of PPO of similar molecular weight is associated with ionic motions. One thing to add is that the existence of both DC conduction and an ionic relaxation peak implies that the ions contributed to the conductance in two ways, partly by long-range diffusion, partly by local fluctuation related to segmental motion.

The inset of Fig. 1 shows Arrhenius plots for both relaxation processes. The three data points appear to obey a linear relation and to be parallel, for both pure PPO melt and PPO with added salt. The implied activation energy is 48 kJ mol^{-1} K^{-1}. To observe the same temperature dependence in both systems supports the idea that although the absolute frequencies characterizing these relaxation processes changed as ions were added, the activation barrier to switch from one state to another did not.

Alternatively, we may probe this system by measuring the diffusion of a fluorescent molecule embedded at dilute concentration within the polymer matrix. Since the probe that we used had a positive charge, it may associate with negatively charged ClO_4^- ions. Therefore, the microviscosity measured by this fluorescent probe gives information about the local environment of ClO_4^- ions. The chemical structure of this probe, rhodamine123, is shown in the upper panel of Fig. 2. The fluorescence depolarization of this fluorescent dye was measured on the nanosecond time scale. Anisotropy, r, is defined as

$$r \equiv (I_{VV} - GI_{VH})/(I_{VV} + 2GI_{VH}) \quad (1)$$

where G is a compensating factor for the signals obtained with different polarization as described elsewhere [16], I is intensity, the first subscript refers to the laser polarization, and the second subscript refers to the direction of fluorescence polarization. For example, I_{VH} is the intensity

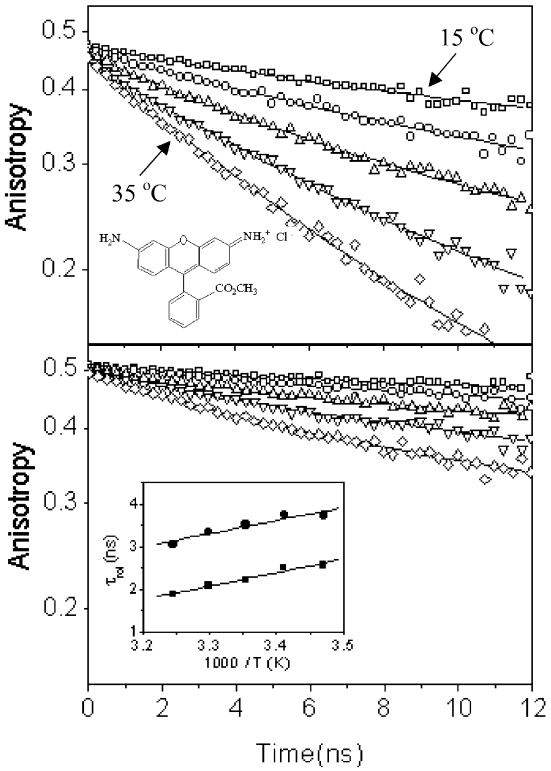

Fig. 2. Fluorescence anisotropy of rhodamine123 is plotted logarithmically against time at various temperatures when the probe was embedded at dilute concentration in a matrix of pure PPO (top panel) and in a matrix of PPO containing 1% Li^+/PPO repeating units (bottom panel). All curves were fitted with first order exponential functions. 15 °C (□); 20 °C (○); 25 °C (△); 30 °C (▽) and 35 °C (◇). Inset (upper panel) shows the chemical structure of the fluorescent dye, rhodamine123. Inset (lower panel) shows an Arrhenius plot for the rotational correlation time of the probe molecules with salt (■) and without salt (•). The deviations of the fits of these curves from linearity, in spite of the first-order exponential fits, reflect the influence of background fluorescence.

of horizontally-polarized fluorescence excited by a vertically-polarized laser beam.

Fig. 2 shows the effect of temperature. As temperature decreased, the rate of fluorescence depolarization slowed, which signifies that the local microviscosity near the probe molecule increased. The deviations of the fits of these curves from linearity, in spite of the first-order exponential fits, reflect the influence of background fluorescence. The case of PPO with added salt displayed slower decay than without added salt, consistent with the dielectric responses in Fig. 1. These decays of fluorescence polarization could be well fitted with first order exponential functions, but the fits were not robust because the decay was small over the available time scales. For definitive characterization, a probe with longer fluorescence lifetime is needed in future work. The inset of lower panel in Fig. 2 shows Arrhenius plots for both rotational processes. The anisotropy decays were well fitted with first order exponential functions ($y = a\exp(-t/\tau) + b$) using a PicoQuant FluoFit software (PicoQuant GmbH). First, the decay curves of pure PPO were fitted without any restriction. However, the decay

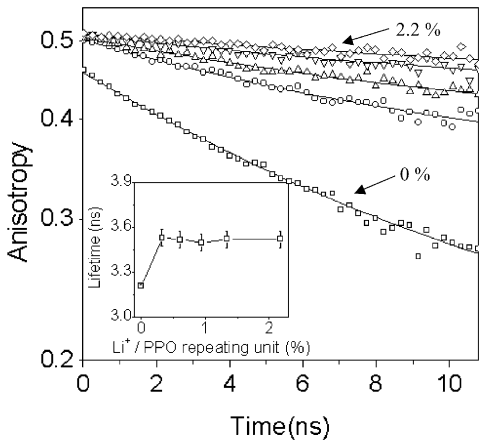

Fig. 3. Fluorescence anisotropy of rhodamine123 is plotted logarithmically against time at various lithium ion concentrations and 25 °C. The ratio of Li^+/PPO repeating units is 0% (□); 0.3% (○); 0.6% (△); 1.3% (▽) and 2.2% (◇). Inset shows the corresponding fluorescence lifetime, plotted linearly against salt concentration.

curves of PPO with salt were fitted with fixed b values from the fitting result of pure PPO at the same temperature to compare with each other since b and τ are highly correlated. The activation energy is 26 kJ mol^{-1} K^{-1} for both cases. Again, the same temperature dependence supports that their microenvironments of the probe molecules are the same regardless of the presence of ions.

Fig. 3 shows the dependence on salt concentration. Fluorescence depolarization is plotted against time on nanosecond time scales. Even with the smallest amounts of added salt, the anisotropy decays were significantly retarded from the case of pure PPO. The smallest concentration was about 3 ions per 1000 PPO repeating units, corresponding to one ion per five PPO molecules. In seeking to interpret this, we note that although the number of charge carriers increased with increasing salt concentration, their mobility (as measured by the dielectric response) decreased, owing to heightened viscosity. Fig. 4 shows the fluorescence depolarization decay time constant

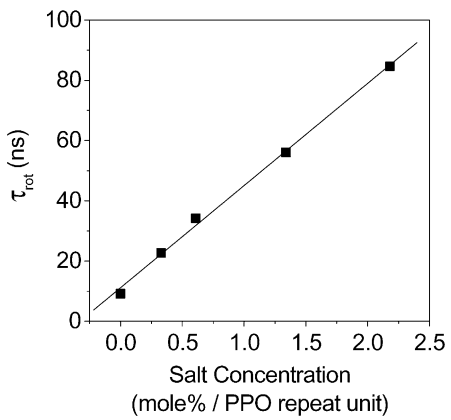

Fig. 4. Rotational time constant, inferred from the fluorescence depolarization decay kinetics, is plotted as a function of $LiClO_4$ concentration (mol% PPO per PPO repeat unit) in the PPO matrix.

plotted against salt concentration. The depolarization time constant appeared to slow down linearly with increasing salt concentration.

The inset of Fig. 3 shows the fluorescence lifetime decay of the dye at different concentrations within the polymer matrix. Lifetime is known to be sensitive to the environment of a fluorescent probe. The fluorescence lifetime increased slightly with the addition of a finite amount of salt and then was constant, regardless of the salt concentration, because the number of ClO_4^- ions at the lowest concentration was already 500 000 times higher than that of the fluorescent probe. This implies that positively charged rhodamine123 interacted with ClO_4^- ions. Fluorescence excitation spectra (not shown here) were also taken. The peak emission changed as salt was added, confirming the interaction between the probe and ClO_4^- ions.

In summary, a combination of dielectric spectroscopy and time-resolved fluorescence depolarization has been used, for the first time to the best of our knowledge, to study local mobility within an ion-conducting polymer. Both measurements showed that the activation energies for the relaxation process of polymer chains and the micromobility of the probe molecules were not affected by the addition of salt while the energy barrier for both processes increased with the addition of salt. Since the electric conductance is the outcome of balance between concentration of ions and their mobility, it is important to understand this local mobility, to which we refer in the title of this Communication as ‘microviscosity’.

Acknowledgments

This work was supported by the US Department of Energy, Division of Materials Science under Award No. DEFG02-91ER45439, through the Frederick Seitz Materials Research Laboratory at the University of Illinois at Urbana–Champaign.

References

[1] McCallum J, Vincent C, Polymer electrolytes review-1, vol. 173. London: Elsevier; 1987.
[2] Donoso J, Bonagamba T, Panepucci H, Oliveira L, Gorecki W, Berthier C, Armand M. J Chem Phys 1993;98:10026.
[3] Tsuchida E, Kobayashi N, Ohno H. Macromolecules 1988;21:96.
[4] Furukawa T, Imura M, Yuruzume H. Jpn J Appl Phys 1997;36:1119.
[5] McLin M, Angell A. Polymer 1996;37:4713.
[6] Furukawa T, Yoneya K, Takahashi Y, Ito K, Ohno H. Electrochim Acta 2000;45:1443.
[7] Watanabe M, Ikeda J, Shinohara I. Polym J 1983;15:65.
[8] Mao G, Perea R, Howells W, Price D, Saboungi M. Nature 2000;405:163.
[9] Inoue S, Kimura Y, Ito K, Hayakawa R. Jpn J Appl Phys 1999;38:L665.
[10] Baur M, Stockmayer W. J Chem Phys 1965;43:4319.
[11] Niclo E, Nicolai T, Durand D. Macromolecules 1999;32:7530.
[12] Kojio K, Jeon S, Granick S. Eur Phys Rev E 2002; in press.
[13] Jeon S, Granick S. Macromolecules 2001;34:8490.
[14] Jeon S, Kwon K, Char K, Granick S. J Poly Sci B in press.
[15] Cho Y-K, Watanabe H, Granick S. J Chem Phys 1999;110:9688.
[16] Jeon S, Bae SC, Granick S. Macromolecules 2001;34:8401.